Backstepping Stabilization of the Linearized *Saint-Venant-Exner* Model: Part II– Output feedback

Ababacar Diagne, Mamadou Diagne, Shuxia Tang and Miroslav Krstic

Abstract— We consider a coupled Saint-Venant-Exner (SVE) model introduced in a companion paper. This studied model describes the water dynamics in a sediment-filled canal with arbitrary values of canal bottom slope, friction, porosity, and water-sediment interaction under subcritical or supercritical flow regime. It consists of two rightward and one leftward convecting transport Partial Differential Equations (PDEs). A single boundary input control (with actuation located only at downstream) strategy is adopted and the backstepping approach developed for the first order linear hyperbolic PDEs is used. A full state feedback exponentially stabilizing controller is designed in the companion paper. In this paper, we first design an exponentially convergent Luenberger observer. Then, based on the full state controller and reconstruction of the distributed state from the observer, we achieve output feedback exponential stabilization of the model.

I. INTRODUCTION

The SVE model, which describes a strong liquid-sediment interaction, has attracted considerable attention over the past decades. Several theoretical and experimental studies have been proposed in the literature, considering the flow and sediment characteristics of the water motion. These studies also addressed the influence of the particle size, shape and density. However, the control of such systems, modeled by nonlinear hyperbolic PDEs, is left out in most of the studies.

Very recently, [1] proposed a singular perturbation approach for the synthesis of boundary control for hyperbolic systems. The effectiveness of the controller is illustrated using the linearized SVE model. In [2] explicit boundary dissipative conditions are given for the exponential stability in $\mathscr{L}^2$-norm of one dimensional linear hyperbolic systems of balance laws. The proposed Lyapunov approach is applied to the linearized SVE equations with successful results. However, on-line measurements of the water levels at both ends of the spatial domain, namely, at upstream ($x = 0$) and downstream ($x = L$) are assumed to be available. Later on, a priori estimation technique and the Faedo-Galerkin method are proposed in [3] for the design of a linear feedback control law that requires only downstream measurements.

In this paper, using the backstepping design [4], [5], [6], we achieve exponential stabilization of the coupled SVE model presented in [2] and discussed widely in the companion paper [6]. A single boundary input control strategy (with

Ababacar Diagne is with Division of Scientific Computing, Department of Information Technology, Uppsala University, Box 337, 75105 Uppsala, Sweden ababacar.diagne@it.uu.se

Mamadou Diagne, Shuxia Tang and Miroslav Krstic are with the Department of Mechanical & Aerospace Engineering, University of California, San Diego, La Jolla, CA 92093-0411 mdiagne@ucsd.edu, sht015@ucsd.edu and krstic@ucsd.edu

actuation located only at downstream) is adopted. A backstepping output feedback controller is designed based on the reconstruction of the distributed state with an exponentially convergent Luenberger observer. We employ a sole sensor at the upstream ($x = 0$) to derive this observer, which estimates the distributed system over the domain. The Froude number is set to $Fr = 1.6$. As a consequence, the flow regime is supercritical (torrential), in other words, all the information of the fluid part travel downwards. With the backstepping method, we achieve the exponential stability results without imposing any conditions in contrast to [2].

II. THE SAINT-VENANT-EXNER MODEL

We consider stabilizing the SVE model around a steady-state using an output feedback backstepping controller. The full description of the physical model defined below, is detailed in the companion paper [6].

$$\frac{\partial H}{\partial t} + V\frac{\partial H}{\partial x} + H\frac{\partial V}{\partial x} = 0 \tag{1a}$$

$$\frac{\partial V}{\partial t} + V\frac{\partial V}{\partial x} + g\frac{\partial H}{\partial x} + g\frac{\partial B}{\partial x} = gS_b - C_f\frac{V^2}{H} \tag{1b}$$

$$\frac{\partial B}{\partial t} + aV^2\frac{\partial V}{\partial x} = 0. \tag{1c}$$

III. PRELIMINARIES

A. Linearized model

Here, we recall briefly the abstract formulation of the linearized version of (1). The derivation of the following representation is fully described in our companion paper [6].

$$\partial_t u_1 + \gamma_1 \partial_x u_1 = \sigma_{11} u_1 + \sigma_{12} u_2 + \alpha_1 v \tag{2a}$$

$$\partial_t u_2 + \gamma_2 \partial_x u_2 = \sigma_{21} u_1 + \sigma_{22} u_2 + \alpha_1 v \tag{2b}$$

$$\partial_t v - \mu \partial_x v = \eta_1 u_1 + \eta_2 u_2 + \alpha_1 v. \tag{2c}$$

Introducing, $w(t,x) = v(t,x)\exp\left(-\frac{\alpha_1}{\mu}x\right)$, we tranform (2) into

$$\partial_t u_1 + \gamma_1 \partial_x u_1 = \sigma_{11} u_1 + \sigma_{12} u_2 + \alpha(x)w \tag{3a}$$

$$\partial_t u_2 + \gamma_2 \partial_x u_2 = \sigma_{21} u_1 + \sigma_{22} u_2 + \alpha(x)w \tag{3b}$$

$$\partial_t w - \mu \partial_x w = \theta_1(x)u_1 + \theta_2(x)u_2 \tag{3c}$$

with $\alpha(x) = \alpha_1 \exp\left(\frac{\alpha_1}{\mu}x\right)$ and $\theta_j(x) = \alpha_{j+1}\exp\left(\frac{\alpha_1}{\mu}x\right)$ for $j = 1, 2$, and the boundary and initial conditions are

$$u_i(t,0) = q_i w(t,0) \quad \text{for i} = 1,2, \tag{4a}$$

$$w(t,1) = \rho_1 u_1(t,1) + \rho_2 u_2(t,1) + U(t), \tag{4b}$$

$$w(0,x) = w^0(x), \, u_i(0,x) = u_i^0(x) \quad \text{for i} = 1,2. \tag{4c}$$

As shown in the companion paper [6] (Theorem 1), the following state feedback controller

$$U(t) = -\rho_1 u_1(t,1) - \rho_2 u_2(t,1) + \int_0^1 \Big[k_1(1,\xi) u_1(x,\xi)$$
$$+ k_2(1,\xi) u_2(x,\xi) + k_3(1,\xi) w(1,\xi) \Big] d\xi, \qquad (5)$$

stabilizes the system (3) with the boundary and initial conditions (4) to the origin. The function k_i are the solutions of the gain kernel PDEs obtained after the transformation of (3) into a suitable target system (see [6]).

Remark 1: We recover a useful classification of flows, based on the dimensionless Froude number defined as

$$Fr = \frac{V^*}{\sqrt{gH_*}}.$$

Let us mention that in the case where the flow regime is supercritical $(F_r > 1)$, the following changes of variable will be considered regarding on the characteristics (see the companion paper [6], section *C. Change of notations*) $v(t,x) = \xi_2(t,x)$, $u_1(t,x) = \xi_1(t,x)$, $u_2(t,x) = \xi_3(t,x)$ and coefficients $\lambda_2 = -\mu$, $\lambda_1 = \gamma_1$ and $\lambda_3 = \gamma_2$.
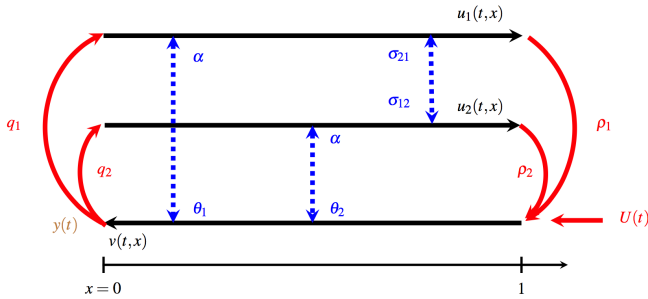

Fig. 1.   Schematic steep of the hyperbolic system.

Here, u_1, u_2 and w are the distributed states and $U(t)$ is the control input as shown in Figure 1. The measured output is given by: $w(t,0) = y(t)$.

B. Backstepping state feedback controller design

We employ the following backstepping transformation

$$\psi_i(t,x) = u_i(t,x) \text{ for } i = 1, 2 \qquad (6)$$

$$\chi(t,x) = w(t,x) - \int_0^x k_1(x,\xi) u_1(t,\xi) d\xi$$
$$- \int_0^x k_2(x,\xi) u_2(t,\xi) d\xi - \int_0^x k_3(x,\xi) w(t,\xi) d\xi. \qquad (7)$$

in which the functions k_i satisfy the following system of first order well-posed hyperbolic PDEs:

$$\mu \partial_x k_1(x,\xi) - \gamma_1 \partial_\xi k_1(x,\xi)$$
$$= \sigma_{11} k_1(x,\xi) + \sigma_{21} k_2(x,\xi) + \theta_1(\xi) k_3(x,\xi) \qquad (8a)$$
$$\mu \partial_x k_2(x,\xi) - \gamma_2 \partial_\xi k_2(x,\xi)$$
$$= \sigma_{12} k_1(x,\xi) + \sigma_{22} k_2(x,\xi) + \theta_2(\xi) k_3(x,\xi) \qquad (8b)$$
$$\mu \partial_x k_3(x,\xi) + \mu \partial_\xi k_3(x,\xi)$$
$$= \alpha(\xi) k_1(x,\xi) + \alpha(\xi) k_2(x,\xi) \qquad (8c)$$

with the following boundary conditions:

$$k_1(x,x) = -\frac{\theta_1(x)}{\gamma_1 + \mu}, \ k_2(x,x) = -\frac{\theta_2(x)}{\gamma_2 + \mu}, \qquad (9a)$$
$$\mu k_3(x,0) = q_1 \gamma_1 k_1(x,0) + q_2 \gamma_2 k_2(x,0). \qquad (9b)$$

Then, the transformation (6)-(7) maps the system (3)-(4) to the exponentially stable target system

$$\partial_t \psi_1 + \gamma_1 \partial_x \psi_1 = \sigma_{11} \psi_1 + \sigma_{12} \psi_2 + \alpha(x) \chi$$
$$+ \int_0^x c_{11}(x,\xi) \psi_1(t,\xi) d\xi$$
$$+ \int_0^x c_{12}(x,\xi) \psi_2(t,\xi) d\xi$$
$$+ \int_0^x \kappa_1(x,\xi) \chi(t,\xi) d\xi \qquad (10a)$$
$$\partial_t \psi_2 + \gamma_2 \partial_x \psi_2 = \sigma_{21} \psi_1 + \sigma_{22} \psi_2 + \alpha(x) \chi$$
$$+ \int_0^x c_{21}(x,\xi) \psi_1(t,\xi) d\xi$$
$$+ \int_0^x c_{22}(x,\xi) \psi_2(t,\xi) d\xi$$
$$+ \int_0^x \kappa_2(x,\xi) \chi(t,\xi) d\xi \qquad (10b)$$
$$\partial_t \chi - \mu \partial_x \chi = 0 \qquad (10c)$$

with the following boundary conditions:

$$\psi_i(t,0) = q_i \chi(t,0) \text{ for } i = 1, 2 \text{ and } \chi(t,1) = 0. \qquad (11)$$

The functions $c_{ij}(\cdot)$ and $\kappa_i(\cdot)$, $i, j = 1, 2$ are

$$c_{ij}(x,\xi) = \alpha(x) k_j(x,\xi) + \int_\xi^x \kappa_i(x,s) k_j(s,\xi) ds \qquad (12)$$

$$\kappa_i(x,\xi) = \alpha(x) k_3(x,\xi) + \int_\xi^x \kappa_i(x,s) k_3(s,\xi) ds, \qquad (13)$$

defined on the triangular domain

$$\mathbb{T} = \Big\{ (x,\xi) \in \mathbb{R}^2 \,|\, 0 \le \xi \le x \le 1 \Big\}.$$

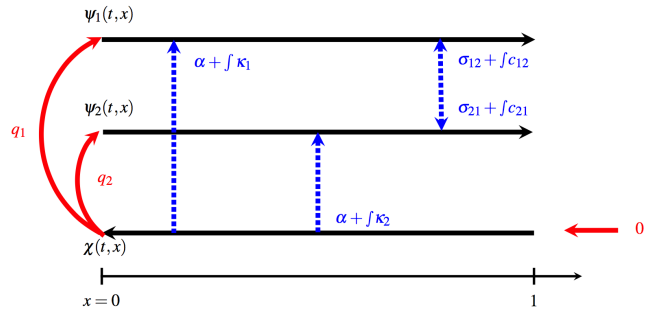The dynamic the target system is represented on Figure 2.

Fig. 2.   Representation of the target system.

C. Inverse transformation and control law

To ensure that the target system and the closed-loop system have equivalent stability properties, the transformation

(6)-(7) has to be invertible. Since $\psi_i = u_i$, for $i = 1, 2$, the transformation (7) can be rewritten as

$$\chi(t,x) + \int_0^x k_1(x,\xi)\psi_1(t,\xi)\,d\xi + \int_0^x k_2(x,\xi)\psi_2(t,\xi)\,d\xi$$
$$= w(t,x) + \int_0^x k_3(x,\xi)w(t,\xi)\,d\xi. \tag{14}$$

Let us define

$$\Gamma(t,x) = \chi(t,x) + \int_0^x k_1(x,\xi)\psi_1(t,\xi)\,d\xi$$
$$+ \int_0^x k_2(x,\xi)\psi_2(t,\xi)\,d\xi \tag{15}$$

Since k_3 is continuous by Theorem 5.3 in [4], there exists a unique continuous inverse kernel l_3 defined on $\mathbb{T}$, such that

$$w(t,x) = \Gamma(t,x) + \int_0^x l_3(x,\xi)\Gamma(t,\xi)\,d\xi, \tag{16}$$

which yields the following inverse transformation Since $\psi_i = u_i$, for $i = 1, 2$, we could get the following relation from the first two equalities of (3) and (10):

$$\alpha(x)w = \alpha(x)\chi + \int_0^x c_{11}(x,\xi)\psi_1(t,\xi)\,d\xi$$
$$+ \int_0^x c_{12}(x,\xi)\psi_2(t,\xi)\,d\xi + \int_0^x \kappa_1(x,\xi)\chi(t,\xi)\,d\xi. \tag{17}$$

Thus, we could write the following

$$w(t,x) = \chi(t,x) + \int_0^x l_1(x,\xi)\psi_1(t,\xi)\,d\xi$$
$$+ \int_0^x l_2(x,\xi)\psi_2(t,\xi)\,d\xi + \int_0^x l_3(x,\xi)\chi(t,\xi)\,d\xi, \tag{18}$$

where for $i = 1, 2$,

$$l_i(x,\xi) = k_i(t,\xi) + \int_\xi^x k_i(x,\xi)l_3(\xi,s)\,ds. \tag{19}$$

Thus, the control law $U(t)$ can be obtained by plugging the transformation (7) into (3). Readily, $\chi(t,1) = 0$ implies that

$$U(t) = -\rho_1 u_1(t,1) - \rho_2 u_2(t,1) + \int_0^1 \Big[k_1(1,\xi)u_1(x,\xi)$$
$$+ k_2(1,\xi)u_2(x,\xi) + k_3(1,\xi)w(1,\xi) \Big]\,d\xi. \tag{20}$$

The k_i in the integral term designate the kernel functions and satisfy the system (8)-(9).

IV. BACKSTEPPING OBSERVER DESIGN

The feedback controller (20) requires a full state measurement across the spatial domain. In this section we are interested in the design of a boundary state observer for estimation of the distributed states of the system (3)-(4) over the whole spatial domain using the measured output $w(t,0) = y(t)$. The observer

$$\partial_t \hat{u}_1 + \gamma_1 \partial_x \hat{u}_1 = \sigma_{11}\hat{u}_1 + \sigma_{12}\hat{u}_2 + \alpha(x)\hat{w}$$
$$- p_1(x)[y(t) - \hat{w}(t,0)] \tag{21a}$$
$$\partial_t \hat{u}_2 + \gamma_2 \partial_x \hat{u}_2 = \sigma_{21}\hat{u}_1 + \sigma_{22}\hat{u}_2 + \alpha(x)\hat{w}$$
$$- p_2(x)[y(t) - \hat{w}(t,0)] \tag{21b}$$
$$\partial_t \hat{w} - \mu \partial_x \hat{w} = \theta_1(x)\hat{u}_1 + \theta_2(x)\hat{u}_2$$
$$- p_3(x)[y(t) - \hat{w}(t,0)], \tag{21c}$$

where $(\hat{u}_1, \hat{u}_2, \hat{w})^T$ is the estimated state vector, consists of a copy of the plant plus an output injection and mimics the well-known finite dimensional observer format. The functions $\theta_j(x) = \alpha_{j+1}$ for $j = 1, 2$ and $\alpha(x)$ are the ones defined for the transformed system (3). The following boundary conditions have to be considered:

$$\hat{u}_i(t,0) = q_i y(t) \quad \text{for } i = 1, 2 \tag{22a}$$
$$\hat{w}(t,1) = \rho_1 \hat{u}_1(t,1) + \rho_2 \hat{u}_2(t,1) + U(t). \tag{22b}$$

Our objective is to find $p_1(x)$, $p_2(x)$ and $p_3(x)$ such that the estimated state vector $(\hat{w}, \hat{u}_1, \hat{u}_2)$ converges to the real state vector (w, u_1, u_2) in finite time. Defining

$$\begin{pmatrix} \tilde{w} & \tilde{u}_1 & \tilde{u}_2 \end{pmatrix}^T = \begin{pmatrix} w - \hat{w} & u_1 - \hat{u}_1 & u_2 - \hat{u}_2 \end{pmatrix}^T \tag{23}$$

as the error variable vector, we obtain the following error system

$$\partial_t \tilde{w} - \mu \partial_x \tilde{w} = \theta_1(x)\tilde{u}_1 + \theta_2(x)\tilde{u}_2 + p_3(x)\tilde{w}(t,0) \tag{24a}$$
$$\partial_t \tilde{u}_1 + \gamma_1 \partial_x \tilde{u}_1 = \sigma_{11}\tilde{u}_1 + \sigma_{12}\tilde{u}_2 + \alpha(x)\tilde{w}$$
$$+ p_1(x)\tilde{w}(t,0) \tag{24b}$$
$$\partial_t \tilde{u}_2 + \gamma_2 \partial_x \tilde{u}_2 = \sigma_{21}\tilde{u}_1 + \sigma_{22}\tilde{u}_2 + \alpha(x)\tilde{w}$$
$$+ p_2(x)\tilde{w}(t,0) \tag{24c}$$

with the boundary conditions

$$\tilde{w}(t,1) = \rho_1 \tilde{u}_1(t,1) + \rho_2 \tilde{u}_2(t,1), \tag{25a}$$
$$\tilde{u}_i(t,0) = 0 \quad \text{for } i = 1, 2. \tag{25b}$$

A. Backstepping transformation and the target error system

Similarly to the controller design, we use the following invertible backstepping transformation

$$\tilde{u}_i(t,x) = \tilde{\pi}_i(t,x) + \int_0^x m_i(x,\xi)\tilde{\phi}(t,\xi)\,d\xi \tag{26a}$$
$$\text{for } i = 1, 2$$
$$\tilde{w}(t,x) = \tilde{\phi}(t,x) + \int_0^x m_3(x,\xi)\tilde{\phi}(t,\xi)\,d\xi, \tag{26b}$$

where the kernels $m_i(\cdot)$ for $i = 1, 2, 3$ are defined in the triangular domain $\mathbb{T}$ to map the error system (24)-(25) into the following exponentially stable target system

$$\partial_t \tilde{\pi}_1 + \gamma_1 \partial_x \tilde{\pi}_1 = \sigma_{11}\tilde{\pi}_1 + \sigma_{12}\tilde{\pi}_2$$
$$+ \int_0^x g_{11}(x,\xi)\tilde{\pi}_1(t,\xi)\,d\xi + \int_0^x g_{12}(x,\xi)\tilde{\pi}_2(t,\xi)\,d\xi \tag{27a}$$
$$\partial_t \tilde{\pi}_2 + \gamma_2 \partial_x \tilde{\pi}_2 = \sigma_{21}\tilde{\pi}_1 + \sigma_{22}\tilde{\pi}_2$$
$$+ \int_0^x g_{21}(x,\xi)\tilde{\pi}_1(t,\xi)\,d\xi + \int_0^x g_{22}(x,\xi)\tilde{\pi}_2(t,\xi)\,d\xi \tag{27b}$$
$$\partial_t \tilde{\phi} - \mu \partial_x \tilde{\phi} = \theta_1(x)\tilde{\pi}_1 + \theta_2(x)\tilde{\pi}_2$$
$$+ \int_0^x h_1(x,\xi)\tilde{\pi}_1(t,\xi)\,d\xi + \int_0^x h_2(x,\xi)\tilde{\pi}_2(t,\xi)\,d\xi \tag{27c}$$

with the boundary conditions

$$\tilde{\pi}_i(t,0) = 0 \text{ for } i = 1, 2 \tag{28a}$$
$$\tilde{\phi}(t,1) = \rho_1 \tilde{\pi}_1(t,1) + \rho_2 \tilde{\pi}_2(t,1). \tag{28b}$$

Here the functions g_{ij} and h_i have to be determined on the triangular domain $\mathscr{T}$. As previously, we are attempting to find some sufficient condition for the kernels to match the target system. Differentiating the transformations (26) in time and space and substituting the results into (24) with the help of (27), the following PDEs are derived for the kernels

$$\gamma_1 \partial_x m_1 - \mu \partial_\xi m_1 = \sigma_{11} m_1 + \sigma_{12} m_2 + \alpha(x) m_3, \quad (29a)$$

$$\gamma_2 \partial_x m_2 - \mu \partial_\xi m_2 = \sigma_{21} m_1 + \sigma_{22} m_2 + \alpha(x) m_3, \quad (29b)$$

$$\mu \partial_x m_3 + \mu \partial_\xi m_3 = -\theta_1(x) m_1 - \theta_2(x) m_2. \quad (29c)$$

To close the writing of the above system, the following boundary conditions are imposed:

$$m_1(x,x) = \frac{1}{\gamma_1 + \mu} \alpha(x), \; m_2(x,x) = \frac{1}{\gamma_2 + \mu} \alpha(x) \quad (30a)$$

$$m_3(1,\xi) = \rho_1 m_1(1,\xi) + \rho_2 m_2(1,\xi). \quad (30b)$$

The observer gains are defined by

$$p_i(x) = \mu m_i(x,0) \text{ for } i = 1, 2, 3, \quad (31)$$

and the integral coupling coefficients are defined by the following equations for $\{i, j\} = 1, 2$

$$h_i(x,\xi) = -\theta(\xi) m_3(x,\xi) - \int_\xi^x m_3(x,s) h_i(s,\xi) \, ds, \quad (32a)$$

$$g_{i,j}(x,\xi) = -\theta_j(\xi) m_i(x,\xi) - \int_\xi^x m_i(x,s) h_j(s,\xi) \, ds. \quad (32b)$$

B. Inverse Transformation

The continuity of the kernel m_3 in the transformation (26b) guarantees the existence of a unique continuous inverse kernel r_3 in the transformation

$$\tilde{\phi}(t,x) = \tilde{w}(t,x) + \int_0^x r_3(x,\xi) \tilde{w}(t,\xi) \, d\xi \quad (33)$$

define on $\mathbb{T}$, and

$$r_3(x,\xi) = -m_3(x,\xi) - \int_\xi^x m_3(x,s) r_3(s,\xi) \, ds. \quad (34)$$

Substituting (34) into (26a), we obtain for $i = 1, 2$,

$$\tilde{\pi}_i(t,x) = \tilde{u}_i(t,x) - \int_0^x m_i(x,\xi) \tilde{w}(t,\xi) \, d\xi$$
$$- \int_0^x \int_0^\xi m_i(x,\xi) r_3(\xi,s) \tilde{w}(t,s) ds d\xi$$
$$= \tilde{u}_i(t,x) - \int_0^x m_i(x,\xi) \tilde{w}(t,\xi) \, d\xi$$
$$- \int_0^x \tilde{w}(t,\xi) \int_\xi^x m_i(x,s) r_3(s,\xi) \, ds d\xi,$$

and hence, for $i = 1, 2$,

$$\tilde{\pi}_i(t,x) = \tilde{u}_i(t,x) + \int_0^x r_i(x,\xi) \tilde{w}(t,\xi) \, d\xi \quad (35)$$

where

$$r_i(x,\xi) = -\tilde{m}_i(x,\xi) - \int_\xi^x m_i(x,s) r_3(s,\xi) \, ds.$$

C. Convergence of the designed observer

We first prove exponential stability of the target error system (27).

Lemma 1: Under the assumptions ψ_1^0, ψ_2^0, $\chi^0 \in \mathscr{L}^2([0,1])$ and g_{ij}, $h_i \in \mathscr{C}(\mathbb{T})$, the system (27) with boundary conditions (28) and given initial condition $(\psi_1^0, \psi_2^0, \chi^0)$ is exponentially stable in the $\mathscr{L}^2$ sense.

Proof 1: The stability proof is based on the time differentiation of the following Lyapunov function

$$V_2(t) = \int_0^1 a_2 e^{-\delta_2 x} \left(\frac{\tilde{\pi}_1^2(t,x)}{\gamma_1} + \frac{\tilde{\pi}_2^2(t,x)}{\gamma_2} \right) dx$$
$$+ \int_0^1 \frac{e^{\delta_2 x}}{\mu} \tilde{\phi}^2(t,x) dx, \quad (36)$$

where a_2 and δ_2 are strictly positive parameters to be determined.

$$\Pi(t,x) = \begin{pmatrix} \tilde{\pi}_1(t,x) \\ \tilde{\pi}_2(t,x) \end{pmatrix}, \; G(x,\xi) = \begin{pmatrix} g_{11}(x,\xi) & g_{12}(x,\xi) \\ g_{21}(x,\xi) & g_{22}(x,\xi) \end{pmatrix},$$
$$\theta(x) = \begin{pmatrix} \theta_1(x) & \theta_2(x) \end{pmatrix}, \; h(x,\xi) = \begin{pmatrix} h_1(x,\xi) & h_2(x,\xi) \end{pmatrix}.$$

Assume that for $\tilde{M} > 0$, we have, $\forall x \in [0,1], \xi \in [0,x]$

$$\|G(x,\xi)\|, \; \|\theta(x)\|, \|h(x,\xi)\| \le \tilde{M}, \quad (37)$$

where the matrix/vector norms $\| \cdot \|$ are compatible with the other corresponding matrix/vector norms. Differentiating this function with respect to time, taking into account of the target error system (27)-(28), integrating by parts and applying Young's inequality at different steps, then we obtain the following inequality:

$$\dot{V}_2(t) \le -e^{-\delta_2} \left[\left(a_2 - 2\rho_1^2 e^{2\delta_2} \right) \tilde{\pi}_1^2(t,1) \right.$$
$$\left. + \left(a_2 - 2\rho_2^2 e^{2\delta_2} \right) \tilde{\pi}_2^2(t,1) \right]$$
$$- \int_0^1 e^{\delta_2 x} \left(\delta_2 - \frac{1+x}{\mu} \right) \tilde{\phi}^2(t,x) \, dx$$
$$- \int_0^1 \Pi^T(t,x) e^{-\delta_2 x} \tilde{P}(x) \, \Pi(t,x) dx, \quad (38)$$

where

$$\tilde{P}(x) = a_2 \left(\delta_2 - \frac{(2+x+1/\delta_2)\tilde{M}}{\varepsilon} \right)$$
$$+ e^{2\delta_2 x} \left(\frac{1}{\delta_2} - 1 \right) \frac{\tilde{M}^2}{\mu} - \frac{\tilde{M}^2}{\delta_2 \mu} e^{\delta_2(1+x)}. \quad (39)$$

First, from (38), we need to choose the tuning parameter $\delta_2 > \frac{1+x}{\mu}$. Then, by choosing

$$a_2 > \max \left\{ 2\rho_1^2 e^{2\delta_2}, 2\rho_2^2 e^{2\delta_2}, \right.$$
$$\left. - \frac{e^{2\delta_2 x} \left(\frac{1}{\delta_2} - 1 \right) \frac{\tilde{M}^2}{\mu} - \frac{\tilde{M}^2}{\delta_2 \mu} e^{\delta_2(1+x)}}{\delta_2 - \frac{(2+x+1/\delta_2)\tilde{M}}{\varepsilon}} \right\} \quad (40)$$

to make sure that the matrix $P(x), x \in [0,1]$ is positive definite, we could derive exponential stability of the target error system.

Then, from the continuity and invertibility of the backstepping transformation (26), we could derive exponential

convergence of the designed observer. Thus, the following theorem is proved.

Theorem 1: Under the assumptions that the initial data are in $\left(\mathscr{L}^2([0,1])\right)^3$, the observer (21) (with the coefficient functions $p_i(x), i = \overline{1,3}$ determined by (29)-(31) and with the boundary condition (22)) exponentially convergent to the system (3) in the $\mathscr{L}^2$ sense.

V. OUTPUT FEEDBACK CONTROL

The controller (20) requires a full state measurement and the observer is designed to reconstruct the state over the whole spatial domain based on an output measurement $w(t, 0)$. Thus, by combining these two, we could design an observer-based output feedback controller.

Theorem 2: Consider the $(u_1, u_2, w)^T$-system (3)-(4) together with the $(\hat{u}_1, \hat{u}_2, \hat{w})^T$-observer (21)-(22). For a given initial condition $(u_1^0, u_2^0, w^0, \hat{u}_1^0, \hat{u}_2^0, \hat{w}^0)^T \in \left(\mathscr{L}^2([0, 1])\right)^6$ and with the control law

$$U(t) = -\rho_1 u_1(t, 1) - \rho_2 u_2(t, 1) + \int_0^1 \Big[k_1(1, \xi)\hat{u}_1(x, \xi) $$
$$+ k_2(1, \xi)\hat{u}_2(x, \xi) + k_3(1, \xi)\hat{w}(1, \xi)\Big] d\xi, \quad (41)$$

where k_1, k_2 and k_3 satisfy (8) with the boundary condition (9), the $(u_1, u_2, w, \hat{u}_1, \hat{u}_2, \hat{w})^T$-system is exponentially stable in the sense of the $\mathscr{L}^2$-norm.

Proof 2: From the definition of the error variable vector (23), the combined closed-loop $(u_1, u_2, w, \hat{u}_1, \hat{u}_2, \hat{w})^T$-system of (3)-(4), (21)-(22) and (41) is equivalent with the $(\hat{u}_1, \hat{u}_2, \hat{w}, \tilde{u}_1, \tilde{u}_2, \tilde{w})^T$-system of (21)-(22), (24)-(25) and (41). In comparison to the backstepping transformation (6) and (7), the invertible transformation

$$\hat{\psi}_i(t, x) = \hat{u}_i(t, x) \text{ for } i = 1, 2 \quad (42)$$

$$\hat{\chi}(t, x) = \hat{w}(t, x) - \int_0^x k_1(x, \xi)\hat{u}_1(t, \xi) d\xi$$
$$- \int_0^x k_2(x, \xi)\hat{u}_2(t, \xi) d\xi$$
$$- \int_0^x k_3(x, \xi)\hat{w}(t, \xi) d\xi \quad (43)$$

and (26) maps the system (21)-(22) into a $(\hat{\psi}_1, \hat{\psi}_2, \hat{\chi}, \tilde{\pi}_1, \tilde{\pi}_2, \tilde{\phi})^T$-system, of which the exponential stability can be proved through the following Lyapunov function:

$$V(t) = \int_0^1 a_1 e^{-\delta_1 x}\left(\frac{\hat{\psi}_1^2(t, x)}{\gamma_1} + \frac{\hat{\psi}_2^2(t, x)}{\gamma_2}\right) dx$$
$$+ \int_0^1 \frac{1+x}{\mu}\hat{\chi}^2(t, x)dx$$
$$+ b\left[\int_0^1 a_2 e^{-\delta_2 x}\left(\frac{\tilde{\pi}_1^2(t, x)}{\gamma_1} + \frac{\tilde{\pi}_2^2(t, x)}{\gamma_2}\right) dx\right.$$
$$\left.+ \int_0^1 \frac{e^{\delta_2 x}}{\mu}\tilde{\phi}^2(t, x)dx\right]. \quad (44)$$

Exponential stability of the $(u_1, u_2, w, \hat{u}_1, \hat{u}_2, \hat{w})^T$-system is thus proved.

VI. NUMERICAL SIMULATIONS

The presented simulation results are performed under a supercritical flow regime and the Froude number is set to $Fr = 1.6$. Using the physical values defined in Table I, and the initial condition of [6], the dynamic of the closed-loop system (2) together with the output feedback control law (43) is simulated. (27)-(28), the kernel PDEs (29)-(30) and the observer gain $p_i(x)$ (Fig. 3) are computed numerically.
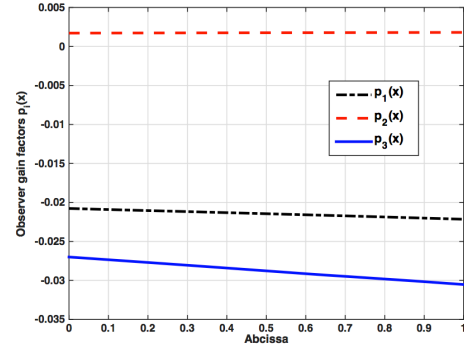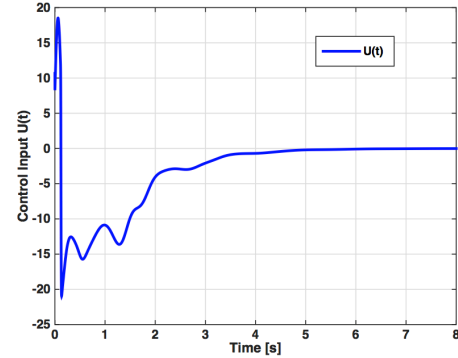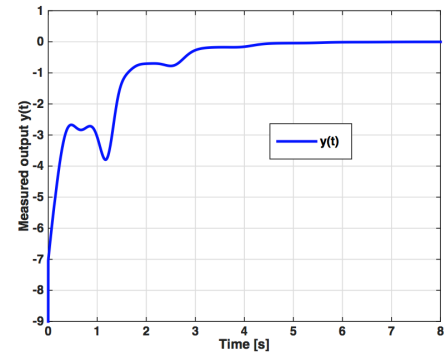

Fig. 3.   Computed observer gains $p_i(x)$.

Figure 4 illustrates the convergences of the input $U(t)$ and the output measurement $y(t)$ to the zero equilibrium after $t = 4s$.
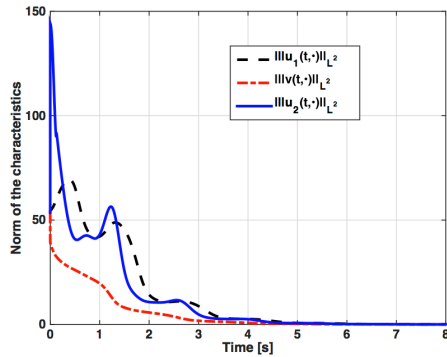

(a) Output control law

(b) Measured output

Fig. 4.   Evolution in time of the control law and the measured output

The dynamic of the $\mathscr{L}^2$-norm is directly related to the magnitude of the propagation speed λ_i as illustrated in Figure

5(a). Actually, the perturbation related to the sediment part takes much more time to vanish than the two others parts.

(a) Ouput feedback control through the backstepping design.
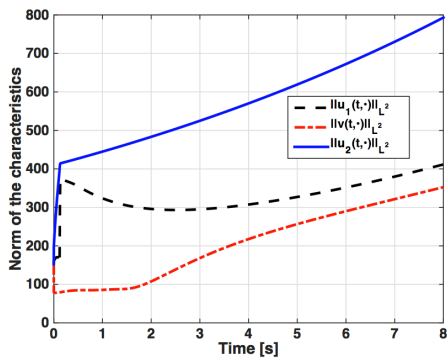
(b) Lyapunov design when the requirements of Theorem 2 in [2] are not fulfilled.

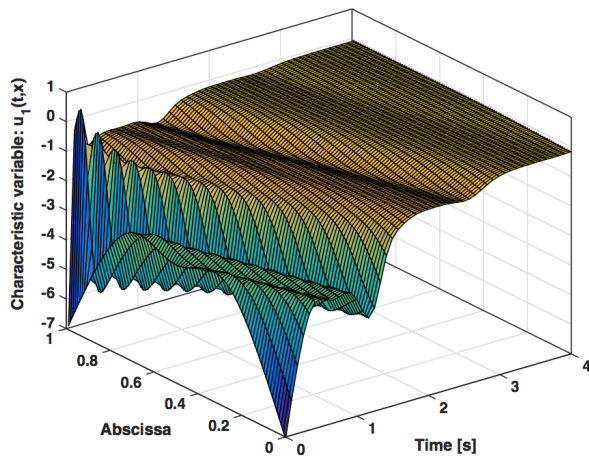Fig. 5.   Evolution in time of the norm of the characteristic solution.

Fig. 6.   Behavior in time and space of the distributed state $u_1(t,x)$.

This class of output feedback controller allows a rapid stabilization of the SVE system, comparing with the results presented in [3] where a boundary measurement scenario is adopted. Figure 5(b) shows that the SVE system blows up under the controller presented in [3] when the backstepping output feedback controller presented in this paper allows the rapid stabilization of the system to the desired setpoint.

Figure 6 illustrates the evolution of the distribute state $u_1(t,x)$ in time and space. The same trend is observed for $u_2(t,x)$ and $v(t,x)$. As can be seen, the simulation results are consistent with the theoritical results presented in this work.

VII. CONCLUSION AND FUTURE WORK

In this paper, a backstepping output feedback controller is designed to achieve the exponential stability of the linearized SVE model. The controller stabilizes the water flow and the bathymetry dynamics at a desired equilibrium set under the supercritical flow regime. The backstepping stabilization is realized with a single downstream boundary control input in contrast to [2], in which exponential stability results was obtained with on-line measurements of the water levels at both ends of the spatial domain. Moreover, simulation results are provided to illustrate that the proposed controller moves beyond the limitations of [2]. In comparison to [2], the backstepping approach offers a more complicated design but enables the exponential stabilization without any restriction, while reducing the number of actuators of the system.

We emphasize that practically, such systems are subjected to several types of perturbations and model uncertainties. Our ongoing works are to consider robustness issues with respect to input matched disturbances [7], [8] for this application.

APPENDIX

T	Δx	CFL	A_g	p_g	C_f	ρ_1	ρ_2
8	0.01	0.9	0.003	0.02	0.1	1	1.5
		q_1	q_2	H^*	U^*	B^*	
		1	1.2	1	5	0.4	

TABLE I

PHYSICAL PARAMETERS AND DIMENSIONLESS NUMBERS

REFERENCES

[1] Y. Tang, C. Prieur, and A. Girard, "Boundary control synthesis for hyperbolic systems: a singular perturbation approach," in *IEEE Conference on Decision and Control, Los Angeles, California, USA*, 2014.

[2] A. Diagne, G. Bastin, and J.-M. Coron, "Lyapunov exponential stability of 1-d linear hyperbolic systems of balance laws," *Automatica*, 2011.

[3] A. Diagne and A. Sène, "Control of shallow water and sediment continuity coupled system," *Mathematics of Control, Signal and Systems (MCSS)*, pp. 387–406, 2013.

[4] F. Di Meglio, R. Vazquez, and M. Krstic, "Stabilization of a system of coupled first-order hyperbolic linear PDEs with a single boundary input," *IEEE Transactions on Automatic Control*, vol. 58, no. 12, pp. 3097–3111, 2013.

[5] M. Krstic and A. Smyshlyaev, *Boundary control of PDEs: A course on backstepping designs*.   Siam, 2008, vol. 16.

[6] A. Diagne, M. Diagne, S. Tang, and M. Krstic, "Backstepping stabilization of the linearized *Saint-Venant-Exner* model: Part I – state feedback approach," in *the 2015 CDC conference, under review*, 2015.

[7] S. Tang and M. Krstic, "Sliding mode control to the stabilization of a linear 2× 2 hyperbolic system with boundary input disturbance," in *American Control Conference (ACC)*.   IEEE, 2014, pp. 1027–1032.

[8] S. Tang, B.-Z. Guo, and M. Krstic, "Active disturbance rejection control for 2×2 hyperbolic systems with input disturbance," in *IFAC World Congress*, 2014, pp. 1027–1032.